Title
A PHENOMENOLOGICAL MODEL FOR A LOCAL REGGE POLE-REGGE CUT INTERACTION

Author
Ghandour, G.I.

Publication Date
1974-04-01

Submitted to Nuclear Physics B ;
also filed as a Ph.D. thesis

LBL-3005
Preprint

A PHENOMENOLOGICAL MODEL FOR A LOCAL REGGE POLE-REGGE CUT INTERACTION

G. I. Ghandour

April 24, 1974

DISCLAIMER

A PHENOMENOLOGICAL MODEL FOR A LOCAL REGGE POLE - REGGE CUT INTERACTION

Contents

	Page
Abstract	1
I. Introduction	2
II. The Effective-Range Formalism	6
III. A Model for $R(j,t)$	13
IV. The Bootstrap Equations at $t = 0$	16
V. Comparison with Experiment	19
V.A. The Effective Trajectory	19
V.B. The Slope Parameter of Proton-Proton Scattering	21
V.C. The Intercept of the Rho Trajectory	25
V.D. The Intercept of the Omega Trajectory	27
VI. Discussion and Conclusion	28
Acknowledgments	30
Appendix A	31
Appendix B	33
Footnotes and References	34
Figure Captions	38
Figures	39

A PHENOMENOLOGICAL MODEL FOR A LOCAL REGGE POLE - REGGE CUT INTERACTION*

G. I. Ghandour+

Department of Physics and Lawrence Berkeley Laboratory
University of California, Berkeley, California 94720

April 24, 1974

ABSTRACT

In the context of the Multiperipheral Model, we use an effective-range approximation and the formula for the discontinuity of the partial wave amplitude across the AFS cut to construct a model amplitude that incorporates the Reggeon-Pomeron cut in addition to the simple Regge pole. We use this amplitude in an attempt to explain the structure of the high energy differential cross section at small t, as observed at ISR. The model explains in addition the discrepancy between the values for the rho-intercept obtained from the differential cross section on the one hand and the difference of $\pi^{\pm}p$ total cross sections, at higher energy, on the other. We can also understand the absence of such a discrepancy in the case of the omega trajectory.

I. INTRODUCTION

The forward angular distribution of pp elastic scattering has been, in recent years, the object of extensive experimental investigations.[1] An interesting phenomenon has been detected, at intersecting storage-ring energies, of a change in slope of the diffraction peak. In the very small t region ($|t| < 0.15$ $(GeV/c)^2$) the slope is, 12 - 13 $(GeV/c)^{-2}$, and then flattens to about 11 $(GeV/c)^{-2}$ in the larger t region ($0.2 < |t| < 0.5$ $(GeV/c)^2$). A similar situation seems to occur at accelerator energies,[2] and possibly in πp elastic scattering,[3] as was pointed out in Ref. 4.

Another interesting phenomenon, this one concerning the intercept of the rho Regge trajectory, has arisen from the Serpukhov data[5] for the total cross section difference

$$\Delta^{\pi p} = \left[\sigma_{tot}^{\pi^- p} - \sigma_{tot}^{\pi^+ p}\right],$$

where a power law fit gives a value[6]

$$\alpha_\rho(0) = 0.68 \pm 0.02 \qquad (I.1)$$

while from differential cross section data for $\pi^- p \to \pi^0 n$, one can extract an effective, linear, rho trajectory[6]

$$\alpha_\rho^{eff}(t) \approx 0.55 + t\,. \qquad (I.2)$$

A discrepancy thus exists between the results of two different determinations of the intercept of the rho trajectory. This discrepancy is compounded by the fact that in the case of the omega Regge trajectory, which is believed to be exchange-degenerate[7] with the rho, the intercept obtained from the difference

$$\Delta^{Kp} = \left[\sigma_{tot}^{K^-p} - \sigma_{tot}^{K^+p}\right] \quad \text{or} \quad \Delta^{pp} = \left[\sigma_{tot}^{p\bar{p}} - \sigma_{tot}^{pp}\right]$$

is close to the value given by (I.2).

Earlier attempts to understand the above phenomena were based on the idea that the relevant Regge trajectory, due to the unitarity effect of a nearby singularity in the partial wave amplitude, exhibits substantial curvature near $t = 0$. Such curvature is indeed expected theoretically[8] from the vicinity of the 2π threshold. However, numerical estimates of this effect on the curvature of the Pomeron[9] and the rho[10] trajectories, owing to the smallness of their coupling to the $\pi\pi$ channel, turned out too small to account for the experimental observations.

A different mechanism for positive curvature of the Pomeron trajectory was anticipated from a particular version of the Multiperipheral Model[11] as a result of interaction between the leading pole and the leading branch point.[12,13] The magnitude of the effect, in this model, is essentially determined by the value of the triple Pomeron coupling. This latter coupling has been estimated by the Deck model[14] and also extracted from experimental data on inclusive reactions.[15,16,17] The value thus obtained was too small for this particular version of the Multiperipheral Model to account for the experimental observations.

In this paper we attempt to explain all the experimental observations presented above as the result of a common phenomenon, namely the interaction between the leading pole and the leading branch point. The emphasis is not only on the curvature of the leading Regge trajectory but also on the fact that, in our model, the pole-cut

interaction turns out to be localized very near $t = 0$. The leading pole and the leading branch point are defined here as in the recent version of the Multiperipheral Model, namely the multifireball expansion.[18,19] Thus, the Pomeron is defined as the mechanism behind the regularities shared by all diffractive processes, at high energy. In a given energy range, it can be simulated by an effective, factorizable, Regge pole.[20] The intercept of this Pomeron is taken to be slightly below one in accordance with Finkelstein-Kajantie.[21] A j-plane amplitude, containing the pole-cut interaction, is constructed by an effective-range type expansion in the combined complex j and t planes, using the formula for the discontinuity across the leading cut as obtained in the Multiperipheral Model.[19,22] Our model is very similar to the version of the Multiperipheral Model mentioned in the previous paragraph[12] but differs from it by the definition and experimental determination of the parameters.

The sign of the Pomeron-Reggeon cut, in our model as in the Multiperipheral Model, is the positive one. Several authors[23,24,25] have proposed a negative sign for the cut, a choice that White[26] has shown to be unavoidable from a mathematical point of view. This, however, does not necessarily contradict our position since the pole and cut we are dealing with are effective ones (appropriate to a finite range of energies), defined from experiment in an operational way and simulating the combined effect of a complicated aggregate of Regge singularities. We will propose an experimental test for this sign in term of the behavior of the intercept of the effective rho trajectory as a function of energy.

The presentation is arranged as follows. In Sec. II, the effective-range formalism is described. An explicit model is suggested in Sec. III. In Sec. IV, the parameters of the leading pole of our model amplitude are bootstrapped in term of some input parameters whose determination from experiment is described in Sec. V. Section VI contains a discussion of the results and the conclusion. The details of some calculations are presented in the Appendices.

II. THE EFFECTIVE-RANGE FORMALISM

We consider the t-channel process

$$P(t_1) + R(t_2) \longrightarrow P(t_3) + R(t_4) \qquad \text{(II.1)}$$

where $P(t)$ and $R(t)$ are respectively Pomeron and Reggeon (Pomeron, rho, etc.) of mass t. We designate by $B(j,t;t_1,t_2,t_3,t_4)$ the appropriate (reduced, definite signature) j-plane amplitude, defined as in the Multiperipheral Model.[18,19,22] We assume, as usual in the Multiperipheral Model, that this amplitude of scattering between Reggeons has the usual properties of real analyticity in the variables j and t, as if the Reggeons were particles. We also assume that this amplitude has a pole at $j = \alpha_R(t)$, corresponding to the exchange of the Reggeon R, and a branch point at $j = \alpha_{PR}(t)$, corresponding to the double exchange of a Pomeron P and a Reggeon R, the PR branch point. The position of this branch point and the discontinuity across the associated cut are given by[19,22]

$$\text{disc}_j\, B(j,t;\, t_1,t_2,t_3,t_4) = \frac{1}{16\pi}\iint \frac{dt'\,dt''}{[-\lambda(t,t',t'')]^{\frac{1}{2}}}\, B(j,t;\, t_1,t_2,t',t'') \times B^*(j,t;\, t',t'',t_3,t_4)\,\delta(j+1-\alpha_P(t')-\alpha_R(t'')) \qquad \text{(II.2)}$$

where $\alpha_P(t)$ and $\alpha_R(t)$ are the Pomeron and Reggeon trajectories, and

$$\lambda(x,y,z) \equiv x^2 + y^2 + z^2 - 2xy - 2yz - 2zx$$

is the usual phase-space factor. The range of integration is such that $\lambda(t,t't'') \leq 0$. The normalization is as in Refs. 27 and 28. We are evidently dealing with the AFS branch point.[23]

Near the pole, we have

$$B(j,t;\, t_1,t_2,t_3,t_4) \underset{j\to\alpha_R(t)}{\sim} \frac{g(t;\, t_1,t_2)\, g(t;\, t_3,t_4)}{j - \alpha_R(t)} \tag{II.3}$$

where $g(t;\, t_1,t_2)$ is the (Pomeron-Reggeon)-Reggeon, (PR)R, vertex function.[14]

The key assumption which allows us to carry out the effective range approach is that the dependence of our amplitude on the masses of the external Reggeons, for j near $\alpha_R(t)$, factors out in the following manner:

$$B(j,t;\, t_1,t_2,t_3,t_4) \approx g(t_1,t_2)\, B(j,t)\, g(t_3,t_4)\,, \tag{II.4}$$

where $g(t_1,t_2)$ is like an "off-mass-shell" form factor, normalized by

$$g(0,0) = 1 \tag{II.5}$$

and $B(j,t)$ is the amplitude when all the external Reggeons have zero masses. Such factorization may be obtained from (II.3) if $g(t;\, t_1,t_2)$ factors accordingly. Now

$$B(j,t) \underset{j\to\alpha_R(t)}{\sim} \frac{g^2(t)}{j - \alpha_R(t)} \tag{II.6}$$

where $g(0)$ is related to $g_{PR,R}$ of Ref. 14 by

$$g^2(0) = \frac{1}{16\pi}\, g^2_{PR,R}\,. \tag{II.7}$$

Equation (II.2) can now be written in the form

$$\operatorname{disc}_j B^{-1}(j,t) = -\rho(j,t) \tag{II.8}$$

where

$$\rho(j,t) = \iint \frac{dt'\, dt''}{[-\lambda(t,t',t'')]^{\frac{1}{2}}}\, g^2(t',t'')\, \delta(j + 1 - \alpha_P(t') - \alpha_R(t''))\,. \tag{II.9}$$

We consider now the function

$$R(j,t) = \frac{1}{\pi} \int_{-\infty}^{\alpha_c(t)} \frac{dj'}{j - j'}\, \rho(j',t)$$

$$= \frac{1}{\pi} \iint \frac{dt'\, dt''}{[-\lambda(t,t',t'')]^{\frac{1}{2}}}\, \frac{g^2(t',t'')}{j + 1 - \alpha_P(t') - \alpha_R(t'')} \tag{II.10}$$

where the delta function has been used to perform the j' integration. This function has the same branch point, in the complex j-plane, as does $B^{-1}(j,t)$, and its discontinuity across the associated cut is such as to cancel that of $B^{-1}(j,t)$ so that the function defined by

$$Y(j,t) = B^{-1}(j,t) + R(j,t) \tag{II.11}$$

does not have the branch point. We expand this function in a power series around $t = 0$ and $j = \alpha_R(0)$, keeping only the linear terms. We write this expansion in the form

$$Y(j,t) \approx \frac{1}{\gamma_R^{\,0}}\, [j - \alpha_R^{\,0}(t)] \tag{II.12}$$

where

$$\alpha_R^{\,0}(t) = 1 - x_R^{\,0} + b_R^{\,0}\, t \tag{II.13}$$

and $\gamma_R^{\,0}$, $x_R^{\,0}$, and $b_R^{\,0}$ are real. These are the parameters of the model.

Substituting (II.12) into (II.11) we get

$$B(j,t) \approx \frac{\gamma_R^0}{j - \alpha_R^0(t) - \gamma_R^0 R(j,t)} . \qquad (II.14)$$

If $R(j,t)$ consists of a regular part in addition to the singular part containing the branch point, only the singular part needs to be substituted in (II.14). The regular part gets absorbed in $Y(j,t)$.

The trajectory $\alpha_R(t)$ is obtained from (II.14) by solving for the real zero of the denominator

$$\alpha_R(t) = \alpha_R^0(t) + \gamma_R^0 R(\alpha_R(t),t) . \qquad (II.15)$$

The trajectory $\alpha_R(t)$ coincides with $\alpha_R^0(t)$ if the interaction term $\gamma_R^0 R(j,t)$ were identically zero. Hence, we may call the linear $\alpha_R^0(t)$, the free trajectory, and $\alpha_R(t)$ the interacting trajectory. Also, it will be seen in Sec. V that γ_R^0 is the square of the triple Regge coupling $g_{PR,R}$ at $t \lesssim -0.15$ $(GeV/c)^2$, where the interaction term has almost died away. This coupling is very small compared to the usual couplings of strong interactions.[14,19] Thus, $\alpha_R^0(t)$ can be thought of as the unperturbed form of $\alpha_R(t)$, the perturbation being brought in by the term $\gamma_R^0 R(\alpha_R(t),t)$. The presence of $\alpha_R(t)$ in the perturbation suggests a bootstrap scheme that has been exploited in Ref. 12 and which we will make use of in Sec. IV.

Chew and Snider,[12] using the Multiperipheral Model, have arrived at a form similar to (II.14) for the case when the Reggeon R is a Pomeron. In their model, the multiperipheral kernel is split into two pieces: a low energy component, assumed to be regular, gives

rise to the unperturbed trajectory $\alpha_P^0(t)$, which is linear by assumption; and a singular high energy component produces the perturbation. The high energy component corresponds to the cut and the two components contain the whole story. Analogous to this model is the two-component model first proposed by Wilson[30] and developed by a number of others[31] who used it quite successfully in fitting multiplicity distributions in high-energy hadronic collisions, and which has been recently generalized to the multifireball expansion and the perturbative approach to the Pomeron.[19,32] The Chew-Snider model illustrates how, in the Multiperipheral Model, one does not consider multi-Reggeon cuts separately. Our model, which in fact was inspired by theirs, can be presented using their formalism but, splitting the multiperipheral kernel into a regular piece and an entirely singular one. This amounts to a different definition of $\alpha_P^0(t)$ who now receives contribution from the regular part of their high energy component of the kernel. The linearity of $\alpha_R^0(t)$, in our model, is a consequence of the effective range approximation.

The effective range approach and the closely related N/D method have been, in the past, a valuable tool for use in the energy plane. Recently, they have been used in the j-plane to obtain models for the Pomeron (Refs. 33, 34, 35). Of these, the Ball-Zachariasen[34] model has been formulated within the context of the Multiperipheral Model but, unlike ours, the Pomeron intercept is one and the triple Pomeron vertex vanishes at $t = 0$. An asymptotically self-consistent amplitude with a singularity structure very different from ours has been obtained. In the self-consistent model by Bronzan,[33] the Pomeron trajectory is singular as it collides with the cut. This collision

does not occur in our model, our trajectory being analytic for $t \leq 0$.

While in these models,[33,34,35] the rise of the total cross section[36] as observed at ISR, and later confirmed at NAL, is (or can be) incorporated and attributed to the collision of two singularties producing a double pole at $t = 0$, this point has been bypassed by our model, since we ignore all effects such as secondary real poles, s-channel absorption, and secondary complex poles (the j-plane manifestation of the threshold mechanism[37] for the rising cross section). Whether there is a connection (or an influence) of such mechanisms on the experimental phenomena we are attempting to understand is not clear to us even though some phenomenological fits,[38] based on the dual absorptive model, tend to support such a connection.

Starting with Gribov and Migdal,[38] a class of models,[40,41,42] formulated within the context of Reggeon calculus, has arrived at a form similar to (II.14) in the course of modifying a bare Pomeron propagator. In these models, the sign of the two-Pomeron cut is negative and the intercept of the Pomeron is assumed to be exactly one. Consistency within the model, then, forces the requirement that the triple Pomeron vertex vanishes at $t = 0$. All models that incorporate this requirement were in trouble after Brower and Weis[43] discovered that the Pomeron must, then, decouple from a large number of processes in the forward direction. Escapes from the decoupling arguments were, however, achieved; either by departure from the simple Regge pole nature of the Pomeron;[34] or by the addition of enhanced absorptive correction to the conventional Regge pole contribution;[40] or by the nonlinearity of the Pomeron trajectory, near $t = 0$, that results from Pomeron interactions.[42]

Evidence for the nonvanishing, at $t = 0$, of the triple Pomeron vertex exists from the pion dominance model,[14] and from the recent fit[17] to all available data on $pp \to px$, which indicate that the triple Pomeron coupling shows no tendency to vanish at $t = 0$. Nonvanishing of this vertex, at this point, and an intercept less than one for the Pomeron are vital features in our model.

III. A MODEL FOR $R(j,t)$

In this section we will not attempt to derive an expression for the interaction term $R(j,t)$, since this would require the knowledge of $g(t',t'')$ and the trajectories $\alpha_P(t)$ and $\alpha_R(t)$ appearing in the definition of $R(j,t)$ as given by (II.10). We will instead, as is usually done when selecting an interaction Lagrangian in field theories, use the criterions of simplicity, maniability, and plausibility. The actual justification must eventually come from comparing the model and its predictions with experiment. In the spirit of the effective range approach, however, the model amplitude that results from the choice of $R(j,t)$ must have the beforehand known singularities with their respective strengthes and no other singularity in the region of expected validity of the expansion.

The simplest and most natural choice of $g(t',t'')$ is the one that has already been used in many versions of the Multiperipheral Model[12,13,44]

$$g(t',t'') = \exp\left[\frac{1}{2}(\lambda_P t' + \lambda_R t'')\right] \tag{III.1}$$

where λ_P and λ_R are real numbers associated with the Pomeron and Reggeon trajectories. Using this form in (II.10) we get

$$R(j,t) = \frac{1}{\pi}\iint \frac{dt'\,dt''}{[-\lambda(t,t',t'')]^{\frac{1}{2}}}\;\frac{\exp[\lambda_P t' + \lambda_R t'']}{j+1-\alpha_P(t')-\alpha_R(t'')}\,. \tag{III.2}$$

Next, we use for the trajectories, under the integrals, the linearized approximation

$$\alpha_P(t) \approx 1 - x_P + b_P t \tag{III.3}$$

$$\alpha_R(t) \approx 1 - x_R + b_R t\,. \tag{III.4}$$

We rewrite $R(j,t)$, using the identity[45]

$$\frac{1}{j+1-\alpha_P(t')-\alpha_R(t'')} \equiv \int_0^\infty dy\,\exp[-y(j+1-\alpha_P(t')-\alpha_R(t''))]$$

and the result of the following integration, performed in Appendix A

$$\frac{1}{\pi}\iint \frac{dt'\,dt''}{[-\lambda(t,t',t'')]^{\frac{1}{2}}}\exp[\gamma_P t' + \gamma_R t''] = \frac{1}{\gamma_P+\gamma_R}\exp\left[\frac{\gamma_P\gamma_R\,t}{\gamma_P+\gamma_R}\right]$$

to obtain

$$R(j,t) = \frac{1}{b_P+b_R}\exp\left[\frac{\lambda_P+\lambda_R}{b_P+b_R}(j-\alpha_{PR}(t)) + \frac{\lambda_R b_P^2 + \lambda_P b_R^2}{(b_P+b_R)^2}\,t\right]$$

$$\times \int_{\frac{\lambda_P+\lambda_R}{b_P+b_R}(j-\alpha_{PR}(t))}^\infty \frac{dy}{y}\exp\left[-y - \frac{(\lambda_R b_P - \lambda_P b_R)^2}{(b_P+b_R)^3}(j-\alpha_{PR}(t))\,\frac{t}{y}\right] \tag{III.5}$$

where we have identified the well-known trajectory of the branch point

$$\alpha_{PR}(t) \approx 1 - x_P - x_R + \frac{b_P b_R}{b_P+b_R}\,t\,. \tag{III.6}$$

The singularity of $R(j,t)$ comes from the lower limit of integration. Since our concern here is to obtain an amplitude with only the singularities at $\alpha_R(t)$ and $\alpha_{PR}(t)$, we simplify (III.5) by substituting for j the linearized form of $\alpha_R(t)$ everywhere except at the lower limit of integration. Then we use (see Appendix B)

$$\int_u^\infty \frac{dy}{y} \exp\left[-y - \frac{v}{y}\right] = \sum_{n=0}^{\infty} \frac{v^n}{(n!)^2} (-\ell n\, u)$$

$$+ \text{ terms regular at } u = 0,$$

and keep only the first term $(-\ell n\, u)$, since v is second order small in an expansion where x_P and t are the small parameters. We thus abstract for $R(j,t)$ the model's form

$$\gamma_R^{\,0} R(j,t) \longrightarrow - \epsilon_R^{\,0} e^{\lambda_R^{\,0} t} \ell n(j - \alpha_{PR}(t)) \qquad \text{(III.7)}$$

where

$$\epsilon_R^{\,0} = \frac{\gamma_R^{\,0}}{b_P + b_R} \exp\left(\frac{\lambda_P + \lambda_R}{b_P + b_R} x_P\right) \qquad \text{(III.8)}$$

and

$$\lambda_R^{\,0} = \frac{\lambda_R(b_P^{\,2} + b_R^{\,2}) + 2\lambda_P b_R^{\,2}}{(b_P + b_R)^2} . \qquad \text{(III.9)}$$

Substituting into (II.14) we obtain our model's amplitude

$$B(j,t) = \frac{\gamma_R^{\,0}}{j - \alpha_R^{\,0}(t) + \epsilon_R^{\,0} \exp(\lambda_R^{\,0} t)\, \ell n(j - \alpha_{PR}(t))} . \qquad \text{(III.10)}$$

An amplitude of this type except with a square-root instead of the log-cut, and an arbitrary sign for $\epsilon_R^{\,0}$, has been discussed in Ref. 35.

IV. THE BOOTSTRAP EQUATIONS AT $t = 0$

The first bootstrap equation expresses the fact that the same trajectory $\alpha_R(t)$ which appears in Eq. (III.2) for $R(j,t)$, is given by the leading pole of (III.10). That is

$$\alpha_R(t) - \alpha_R^{\,0}(t) + \epsilon_R^{\,0} e^{\lambda_R^{\,0} t} \ell n[\alpha_R(t) - \alpha_{PR}(t)] = 0 . \qquad \text{(IV.1)}$$

This equation and its first derivative with respect to t give, at $t = 0$

$$x_R - x_R^{\,0} - \epsilon_R^{\,0} \ell n\, x_P = 0 \qquad \text{(IV.2)}$$

$$b_R - b_R^{\,0} + \epsilon_R^{\,0} \lambda_R^{\,0} \ell n\, x_P + \frac{\epsilon_R^{\,0} b_R^{\,2}}{(b_R + b_P)x_P} = 0 \qquad \text{(IV.3)}$$

where the notation is as defined by (II.13), (III.3) and (III.4). Also Eq. (III.6) for the cut has been used here.

The residue of the pole at $\alpha_R(t)$ is

$$\gamma_R(t) = \frac{\gamma_R^{\,0}}{1 + \dfrac{\epsilon_R^{\,0} \exp(\lambda_R^{\,0} t)}{\alpha_R(t) - \alpha_{PR}(t)}} . \qquad \text{(IV.4)}$$

Near $t = 0$, we write

$$\gamma_R(t) \approx \gamma_R \exp(\lambda_R t) . \qquad \text{(IV.5)}$$

The second bootstrap equation expresses the requirement that the same λ_R of (IV.5) also appear in Eq. (III.2) for $R(j,t)$. Thus, at $t = 0$, we get from (IV.4) and its first derivative with respect to t, taking (IV.5) into account

$$\gamma_R = \frac{\gamma_R^0}{1 + \epsilon_R^0/x_P} \tag{IV.6}$$

and

$$\lambda_R = \frac{\epsilon_R^0}{\epsilon_R^0 + x_P}\left[\frac{b_R^2}{(b_P + b_R)x_P} - \lambda_R^0\right] \tag{IV.7}$$

where λ_R^0 is given by (III.9), or

$$\lambda_R^0 = \frac{(b_P^2 + b_R^2)\lambda_R + 2b_R^2\lambda_P}{(b_P + b_R)^2} . \tag{IV.8}$$

From the case when R is also a Pomeron, we get

$$x_P - x_P^0 - \epsilon_P^0 \ln x_P = 0 \tag{IV.9}$$

$$b_P - b_P^0 + \epsilon_P^0 \lambda_P^0 \ln x_P + \frac{\epsilon_P^0 b_P}{2x_P} = 0 \tag{IV.10}$$

$$\lambda_P^0 = \lambda_P = \frac{\epsilon_P^0 b_P}{2(2\epsilon_P^0 + x_P)x_P} \tag{IV.11}$$

$$\gamma_P = \frac{\gamma_P^0}{1 + \epsilon_P^0/x_P} . \tag{IV.12}$$

Of the above two bootstrap conditions the second is somewhat controversial. The two Reggeons R in the (RP,R) vertex may very well play different roles and introduce different t-dependence in the vertex function. Also the approximation involved in getting (IV.8) is somewhat crude, especially when R is different from P. We therefore regard Eq. (IV.8) with caution and leave it to the next section, where the model is compared with experiment, to decide on its value.

If Eq. (IV.8) is taken seriously, then λ_R can be eliminated between (IV.7) and (IV.8) and the λ_R^0 thus obtained can be substituted in (IV.3) to yield for b_R the equation

$$\left[(b_P + b_R)^2 + \frac{\epsilon_R^0}{\epsilon_R^0 + x_P}(b_P^2 + b_R^2)\right]\left[(b_R - b_R^0)(b_P + b_R) + \frac{\epsilon_R^0}{x_P} b_R^2\right]$$

$$- \frac{\epsilon_R^0}{\epsilon_R^0 + x_P}\,\frac{x_R^0 - x_R}{x_P}\,(b_P^2 + b_R^2)b_R^2$$

$$- 2(x_R^0 - x_R)(b_P + b_R)\lambda_P b_R^2 = 0 . \tag{IV.13}$$

If Eq. (IV.8) is not retained, then, b_R would have to be determined by other considerations, as will be seen in the next section.

V. COMPARISON WITH EXPERIMENT

V.A. The Effective Trajectory

Almost all the information that is available to us for the choice of the numerical values of our input parameters is extracted from experimental data using models that incorporate only Regge poles. It is therefore important that we extract, in our model, an effective trajectory which, at a given energy, simulates the combined effect of our pole and cut.

The Mellin transform of $B(j,t)$ for $t < 0$ gives the imaginary part, $A(s,t)$, of the scattering amplitude, $M(s,t)$, above the s-channel threshold

$$A(s,t) = \text{Im } M(s,t) = \frac{1}{2\pi i} \int_{-i\infty+\delta}^{i\infty+\delta} dj\, s^j\, B(j,t)$$

where δ is to the right of all the j-plane singularities of $B(j,t)$. Our amplitude, given by (III.10), has a real pole at $j = \alpha_R(t)$ and a cut running from $j = -\infty$ to $j = \alpha_{PR}(t)$. All other singularities are on the unphysical sheet of the j-plane, therefore, by appropriate modification of the contour of integration, we get

$$A(s,t) = \gamma_R(t)\, s^{\alpha_R(t)} - \frac{1}{\pi} \int_{-\infty}^{\alpha_{PR}(t)} dj\, s^j\, \text{disc}_j\, B(j,t), \qquad \text{(V.A.1)}$$

where the discontinuity of $B(j,t)$ across the j-plane cut, $\text{disc}_j\, B(j,t)$, is obtained from (III.10)

$$\text{disc}_j\, B(j,t) = \frac{-\pi\, \gamma_R^0\, \epsilon_R^0\, e^{\lambda_R^0 t}}{\left[j - \alpha_R^0(t) + \epsilon_R^0\, e^{\lambda_R^0 t}\, \ell n(\alpha_{PR}(t) - j)\right]^2 + \left[\pi \epsilon_R^0\, e^{\lambda_R^0 t}\right]^2}. \qquad \text{(V.A.2)}$$

The effective trajectory and the corresponding effective residue are defined by the relation

$$A(s,t) = \gamma_R^{\text{eff}}(t)\, s^{\alpha_R^{\text{eff}}(t)} \qquad \text{(V.A.3)}$$

or

$$\alpha_R^{\text{eff}}(t) = \frac{\partial}{\partial(\ell n\, s)} \left[\ell n\, A(s,t)\right]. \qquad \text{(V.A.4)}$$

Instead of having one effective pole to simulate the combined pole-cut system, one might be tempted to approximate the cut itself by an effective pole. The location of this pole would be where the discontinuity, given by (V.A.2), has its peak value. This occurs at j solution of the equation

$$j - \alpha_R^0(t) + \epsilon_R^0\, e^{\lambda_R^0 t}\, \ell n(\alpha_{PR}(t) - j) = 0. \qquad \text{(V.A.5)}$$

This equation has in general two real solutions, or none. If it has no real solution, then, the peak of the discontinuity is at the value of j where the derivative with respect to j of the denominator of (V.A.2) vanishes, that is at

$$j = \alpha_{PR}(t) - \epsilon_R^0\, e^{\lambda_R^0 t}. \qquad \text{(V.A.6)}$$

The effective residue, at this effective pole, would be given by the area under the peak, the integrated discontinuity

$$\gamma_{PR}^{eff}(t) = -\frac{1}{\pi}\int_{-\infty}^{\alpha_{PR}(t)} dj\ \mathrm{disc}_j\, B(j,t) . \qquad (V.A.7)$$

Our model amplitude, as given by (III.10), satisfies an unsubtracted dispersion relation in j from which we can abstract a sum rule[12] that the integrated cut discontinuity plus the pole residue is equal to the residue of the unperturbed pole, $\gamma_R^{\,0}$

$$\gamma_R(t) + \gamma_{PR}^{eff}(t) = \gamma_R^{\,0} \qquad (V.A.8)$$

whence a simple expression for $\gamma_{PR}^{eff}(t)$ is obtained.

The interaction term $\epsilon_R^{\,0} \exp(\lambda_R^{\,0} t)\, \ell n(j - \alpha_{PR}(t))$, which appears in (III.10), becomes vanishingly small for $t \lesssim -0.15\ (\mathrm{GeV/c})^2$. This happens because $\epsilon_R^{\,0}$ is very small and $\lambda_R^{\,0}$ is very large, as will be seen in the following subsections. Thus, for $t \lesssim -0.15\ (\mathrm{GeV/c})^2$, we expect the effective trajectory, given by (V.A.4), and the effective residue to reduce to the unperturbed values. We will make use of this point in determining our input parameters from experiment in the following subsections.

V.B. The Slope Parameter of Proton-Proton Scattering

In this case the R trajectory is a Pomeron.

For the unperturbed value of the triple Pomeron coupling we use the result of Ref. 16, extracted from inclusive data at $t = -0.15\ (\mathrm{GeV/c})^2$:

$$g_{PPP}^{0} \approx 0.25\ \mathrm{GeV}^{-1} . \qquad (V.B.1)$$

Hence

$$\gamma_R^{\,0} = \frac{1}{16\pi}\, g_{PPP}^{0\ 2} \approx 1.24 \times 10^{-3}\ \mathrm{GeV}^{-2} \qquad (V.B.2)$$

where the 16π comes from our normalization, as noted in (II.7). Equation (III.8) for $\epsilon_P^{\,0}$ becomes

$$\epsilon_P^{\,0} = \frac{g_{PPP}^{0\ 2}}{32\pi\, b_P} \exp\left(\frac{\lambda_P}{b_P}\, x_P\right) . \qquad (V.B.3)$$

The slope of the Pomeron trajectory, as extracted from the ISR data for proton proton elastic differential cross section,[1] has an average value of $0.37 \pm 0.08\ (\mathrm{GeV/c})^{-2}$ for t in the range $0.05 < |t| < 0.10\ (\mathrm{GeV/c})^2$, and $0.10 \pm 0.06\ (\mathrm{GeV/c})^{-2}$ for t in the range $0.10 < |t| < 0.30\ (\mathrm{GeV/c})^2$. Here we use

$$b_P = 0.3\ (\mathrm{GeV/c})^{-2} \qquad (V.B.4)$$

and

$$b_P^{\,0} = 0.1\ (\mathrm{GeV/c})^{-2} . \qquad (V.B.5)$$

Then we determine x_P and λ_P by (IV.11), (V.B.1) and (V.B.3), we get

$$x_P = 0.002 \qquad (V.B.6)$$

and

$$\lambda_P = 26.11\ (\mathrm{GeV/c})^{-2} . \qquad (V.B.7)$$

Equation (IV.9) then determines $x_P^{\,0}$

$$x_P^{\,0} = 0.016 . \qquad (V.B.8)$$

With $\alpha_P^{\,0}(t)$, $\gamma_P^{\,0}$, $\epsilon_P^{\,0}$ and a linear approximation for $\alpha_{PP}(t)$ determined, our model for the Pomeron trajectory is completly specified. The curvature of the cut trajectory, near $t = 0$, has been

neglected, since it is much smaller than that of the pole trajectory, as can easily be seen from

$$\alpha_{PP}(t) = 2\alpha_P(t/4) - 1 .$$

In Fig. 1 we show the discontinuity of $B(j,t)$ across the j-plane cut, as given by (V.A.2), for $t = 0$. The peak value is at $j = \alpha_{PP}(0) - \epsilon_P^0$. The integrated discontinuity, which is the area under the curve is almost equal to the residue of the Pomeron pole. Thus, at $t = 0$, the Pomeron pole and two-Pomeron cut are equally important, in our model.

So far, the amplitude we wrote was for Pomeron-Reggeon "scattering". The simplest way to obtain a similar amplitude for proton-proton scattering is to use the result of Ref. 12 which amounts to replacing γ_P^0 in the numerator of (III.10) by a t-dependent factor $\gamma_p(t)$, which we parametrize by

$$\gamma_p(t) = \gamma_p \, e^{\lambda_p t} . \qquad \text{(V.B.9)}$$

This term is essentially the square of the Pomeron-proton-proton vertex. Thus, the absorptive part for proton proton scattering is calculated from the absorptive part for Pomeron-Pomeron "scattering" by the relation

$$A_{pp}(s,t) \approx \frac{\gamma_p(t)}{\gamma_P^0} A(s,t) . \qquad \text{(V.B.10)}$$

It follows that the elastic cross section for proton proton has the standard high-energy form

$$\frac{d\sigma_{el}^{pp}}{dt} \sim \left[\frac{\gamma_p(t)}{\gamma_P^0}\right]^2 |A(s,t)|^2 \, |i - \cot \tfrac{1}{2}\pi \alpha_P(t)|^2 \qquad \text{(V.B.11)}$$

where we ignored spin, a simplification legitimate near $t = 0$.

The slope parameter is defined by

$$p = \frac{d}{dt} \ell n \left[\left(\frac{d\sigma}{dt}\right) \Big/ \left(\frac{d\sigma}{dt}\right)_{t=0} \right] . \qquad \text{(V.B.12)}$$

We solve Eq. (IV.1) for $\alpha_P(t)$, then calculate $A(s,t)$ using (V.A.1), and $d\sigma/dt$ using (V.B.11), and finally p using (V.B.12). We use for λ_p the value

$$\lambda_p = 4.75 \ (\text{GeV/c})^{-2} \qquad \text{(V.B.13)}$$

which is obtained by fitting the experimental data on the slope parameter in the outer t-region (the unperturbed region in our model) to the Regge form[1]

$$p = 2\lambda_p + 2\alpha' \ \ell n \ s . \qquad \text{(V.B.14)}$$

In Fig. 2, we show our result for the slope parameter, as a function of t, for $\ell n \, s = 8$. In Fig. 3, we show the same for $\ell n \, s = 6$. The slope parameter, at $t = 0$, is shown in Fig. 4 as $\ell n \, s$ is varied. For $t \lesssim -0.1 \ (\text{GeV/c})^2$ the slope parameter can be calculated from (V.B.14) with $\alpha' = 0.1$. We obtain for the effective Pomeron trajectory, as defined by (V.A.4), the expansion

$$\alpha_P^{eff}(t) \approx 0.99 + 0.25t + 0.75t^2 + \cdots . \qquad \text{(V.B.15)}$$

A qualitative agreement with experiment is thus obtained with our oversimplified model without adjusting any free parameter. However, if we were to relax the second bootstrap condition, we could regard λ_P as a free parameter. Also, the values of the triple Pomeron coupling and the Pomeron slope at $t = 0$, are known only roughly. By

varying λ_P, g^0_{PPP} and b_P within reasonable limits we can improve the agreement of our results with experiment.

V.C. The Intercept of the Rho Trajectory

In this case the R trajectory is a rho.

The unperturbed trajectory is the one obtained by fitting the differential cross section data for $\pi^- p \to \pi^0 n$, in the unperturbed region $-t \gtrsim 0.15$ (GeV/c)^2. We take

$$\alpha_\rho^0(t) = 0.55 + t \,. \qquad \text{(V.C.1)}$$

We determine x_ρ by adjusting the intercept of the effective trajectory, at the Serpukhov energy ($\ell n\, s \sim 5$), to come out to be 0.68 in accordance with (I.1). We find

$$x_\rho = 0.2 \,. \qquad \text{(V.C.2)}$$

The slope of the rho trajectory can, in principle, be obtained from (IV.13). This equation, however, has no real root while $\alpha_R(t)$ is, in our model, essentially real. We therefore abandon, at this point, the second bootstrap condition, and instead concentrate on the requirement that the interaction be localized near $t = 0$. To obtain a large value of λ_ρ^0 we need a negative value of b_ρ such that $|b_\rho| < b_P$. Taking for b_ρ the value

$$b_\rho = -0.2 \text{ (GeV/c)}^{-2} \qquad \text{(V.C.3)}$$

we get for λ_ρ^0, from Eq. (IV.3)

$$\lambda_\rho^0 = 27.38 \text{ (GeV/c)}^{-2} \,, \qquad \text{(V.C.4)}$$

We now determine ϵ_ρ^0, using (IV.2). We get

$$\epsilon_\rho^0 = 0.04 \qquad \text{(V.C.5)}$$

and from (III.8) we obtain

$$\gamma_\rho^0 = \frac{1}{16\pi} g^{0\,2}_{P\rho,\rho} \approx 1.38 \times 10^{-3} \text{ GeV}^{-2} \qquad \text{(V.C.6)}$$

or

$$g^0_{P\rho,\rho} \approx 0.26 \text{ GeV}^{-1} \,. \qquad \text{(V.C.7)}$$

This value of $g^0_{P\rho,\rho}$ is very reasonable when compared to the analogous $g_{PP',P'}$ obtained from the Deck model.[14] There exists no experimental determination of this coupling that we know of.

The discontinuity of $B(j,t)$ across the j-plane cut, for $t = 0$, is shown in Fig. 5. There are two peaks, one of them is between $\alpha_{P\rho}(0)$ and $\alpha_{P\rho}(0) - \epsilon_\rho^0$, the other is between $\alpha_{P\rho}(0) - \epsilon_\rho^0$ and $\alpha_\rho^0(0)$, rather close to $\alpha_\rho^0(0)$. The area under the second peak is the largest and is much larger than the rho residue. Thus, at $t = 0$, the cut dominates over the pole in our model for Pomeron rho "scattering".

The effective rho trajectory, as defined by (V.A.4), is shown in Fig. 6 for $\ell n\, s = 5$ and $\ell n\, s = 3$. Also shown in Fig. 6 is the Serpukhov result for the intercept at $\ell n\, s \sim 5$, and the results for the effective trajectory, as found in Ref. 46, from the experimental data on $\pi^- p \to \pi^0 n$ at $t \lesssim 0$ and $\ell n\, s \sim 2 - 3.5$. The agreement with experiment is satisfactory. The predicted variation with energy of the intercept of this effective trajectory is shown in Fig. 7. The intercept is expected to increase, with increasing energy, until it reaches a saturation value which corresponds to the intercept of the rho trajectory itself.

V.D. The Intercept of the Omega Trajectory

The case of the omega trajectory can be understood, in our model, if the triple Regge coupling $g_{P\omega,\omega}$ is much smaller than $g_{P\rho,\rho}$

$$g_{P\omega,\omega} \ll g_{P\rho,\rho} . \qquad \text{(V.D.1)}$$

That such is indeed the case is expected in the Deck model[14] and in the Multiperipheral Model[45] in general, where the triple Regge couplings are determined, essentially, by the triangle of pions shown in Fig. 8. The coupling of the omega trajectory to two pions is zero because of G-parity conservation.

VI. DISCUSSION AND CONCLUSION

We ignored in this paper the t-channel unitarity effect of the $\pi\pi$ threshold on the Pomeron[9] and the rho[10] trajectories. The combined effect of this threshold and the j-plane cut can be studied by applying the effective range formalism to a coupled two-channel system, the two channels being the PR and the $\pi\pi$ channels. $R(j,t)$ of (III.10) will then contain an additional term due to the $\pi\pi$ threshold, and additional small curvature, near $t = 0$, will be found in the output trajectory.

Although we do not know whether to expect our model to remain valid for positive t, since the choice (III.1) of the form factors is then doubtful, we can speculate that because the pole and branch point widen their separation the perturbation becomes smaller and $\alpha_R(t)$ approaches $\alpha_R{}^0(t)$ as t increases positively.

We used in Sec. V an energy scale factor $s_0 = 1\ \text{GeV}^2$. Thus s must be understood as (s/s_0). A different choice for s_0 can make some difference. For example, were we to choose $s_0 = 0.5\ \text{GeV}^2$, then, our results for $\ell n\ s = 8$ must be read from the results of Sec. V at $\ell n\ s = 8 - \ell n\ s_0 = 8 - \ell n\ 0.5$. Evidently such a change does not make much difference for large values of $\ell n\ s$.

The intercept of the effective rho trajectory is expected, in our model, to increase with increasing energy, until it reaches a saturation value corresponding to the intercept of the rho pole. This behavior is a consequence of our choice of the positive sign for the Pomeron-rho cut. If we were to choose the negative sign, the opposite behavior would be expected. Similar behavior of the intercept of the Pomeron trajectory is also expected, while the experimental results

on the rise of the total cross section seem to invalidate our model. We must remember, however, that lower Regge singularities, which might account for the rise of the total cross section, have been omitted here. Analogous mechanisms can eventually affect the behavior of the intercept of the effective rho trajectory. Thus, we can only say that if the intercept of the effective rho trajectory is seen to increase with energy, then, the negative sign for the effective Pomeron-rho cut would seem to be ruled out.

If the concept of exchange-degenerate trajectories is valid, at relatively low energy, the mechanism displayed by our model seems to break that exchange-degeneracy at higher energy, unless a very appropriate exchange-degeneracy exists between the triple Regge couplings involved. Arguments for such exchange degeneracy have been, so far, either ad hoc or in conflict with G-parity conservation,[47] a principle which also was relevant in our model as the probable reason behind the difference of behavior between the omega and rho trajectories.

We feel that the most interesting aspect of our model is the close relationship between the magnitude of triple Regge couplings and low-t deviations of trajectories from linearity. Definitive measurement of these deviations would yield independent evidence about the corresponding triple Regge couplings.

ACKNOWLEDGMENTS

It is a pleasure to thank Professor G. F. Chew for his patience, guidance, and many interesting ideas, without which this work would not have been possible.

Helpful conversations with R. Shankar and J. Koplik are gratefully acknowledged.

I wish to thank Ms. Georgella Perry for her effort in typing this text.

I am forever indebted to my wife, Leila, for her encouragement and patience.

APPENDIX A

Consider the integral

$$I(t) = \frac{1}{\pi}\iint \frac{dt'\,dt''}{[-\lambda(t,t',t'')]^{\frac{1}{2}}} \exp[\gamma_P t' + \gamma_R t''] \qquad (A.1)$$

where

$$\lambda(t,t',t'') \equiv t^2 + t'^2 + t''^2 - 2tt' - 2tt'' - 2t't''$$

and the range of integration is such that $\lambda(t,t',t'') \leq 0$.

The change of variables[45]

$$t' = u + \frac{t}{4} + [ut]^{\frac{1}{2}} \cos\phi$$

$$t'' = u + \frac{t}{4} - [ut]^{\frac{1}{2}} \cos\phi$$

reduces $I(t)$ to the form

$$I(t) = \frac{1}{\pi}\int_{-\infty}^{0} du \int_{0}^{\pi} d\phi \exp\left[(\gamma_R + \gamma_P)(u + \frac{t}{4}) + (\gamma_R - \gamma_P)[ut]^{\frac{1}{2}} \cos\phi\right]. \qquad (A.2)$$

Then we use

$$\frac{1}{\pi}\int_{0}^{\pi} d\phi \exp\left[(\gamma_R - \gamma_P)[ut]^{\frac{1}{2}} \cos\phi\right] = I_0\left[(\gamma_R - \gamma_P)[ut]^{\frac{1}{2}}\right]$$

where I_0 is a Bessel function. And

$$\int_0^{\infty} dv \exp\left[-(\gamma_R + \gamma_P)(v - \frac{t}{4})\right] I_0\left((\gamma_R - \gamma_P)[-vt]^{\frac{1}{2}}\right)$$

$$= \frac{1}{\gamma_R + \gamma_P} \exp\left[(\gamma_R + \gamma_P)\frac{t}{4} - \frac{(\gamma_R - \gamma_P)^2}{\gamma_R + \gamma_P}\frac{t}{4}\right]$$

$$= \frac{1}{\gamma_R + \gamma_P} \exp\left[\frac{\gamma_R\gamma_P}{\gamma_R + \gamma_P}\, t\right] .$$

APPENDIX B

Consider the integral

$$I(u,v) = \int_u^\infty \frac{dy}{y} \exp\left[-y - \frac{v}{y}\right] . \qquad (B.1)$$

Expanding the second exponential we get

$$I(u,v) = \sum_{n=0}^{\infty} (-1)^n \frac{v^n}{n!} \int_u^\infty \frac{dy}{y^{n+1}} \exp(-y) \qquad (B.2)$$

we have

$$\int_u^\infty \frac{dy}{y^{n+1}} \exp(-y) = \frac{1}{u^n} \int_1^\infty \frac{dt}{t^{n+1}} \exp(-ut)$$

$$= \frac{1}{u^n} E_{n+1}(u) \qquad (B.3)$$

where $E_{n+1}(u)$ is the exponential integral for which we have the handbook expansion

$$E_{n+1}(u) = \frac{(-u)^n}{n!} \left(-\ell n\, u - \mathbb{C} + \sum_{m=1}^{n} \frac{1}{m} - \sum_{\substack{m=0 \\ m\neq n}}^{\infty}{}' \frac{(-u)^m}{(m-n)m!}\right) \qquad (B.4)$$

valid for $|\arg u| < \pi$; $\mathbb{C}$ is the Euler constant $(0.577\cdots)$. Putting it all together, we get

$$I(u,v) = \sum_{n=0}^{\infty} \frac{v^n}{(n!)^2} (-\ell n\, u) + \text{terms regular at } u = 0.$$

FOOTNOTES AND REFERENCES

* This work was supported in part by the U. S. Atomic Energy Commission.

+ CNRS - Lebanon Graduate Fellow.

1. M. Holder, et al., Phys. Lett. 35B, 355 (1971); 36B, 400 (1971); U. Amaldi, et al., Phys. Lett. 36B, 504 (1971); G. Barbiellini, et al., Phys. Lett. 39B, 663 (1972); 35B, 355 (1971); U. Amaldi, et al., paper submitted to the APS Division of Particles and Fields Meeting, Berkeley, August 1973; V. Bartenev, et al., NAL Pub. 73/54 and also submitted to the APS Division of Particles and Fields Meeting, Berkeley, August 1973.
2. G. G. Beznogikh, et al., Phys. Lett. 30B, 274 (1969).
3. K. J. Foley, et al., Phys. Rev. 181, 1775 (1969); K. J. Foley, et al., Phys. Rev. Lett. 15, 45 (1965).
4. R. A. Carrigan, Jr., Phys. Rev. Lett. 24, 168 (1970).
5. S. P. Denisov, et al., Phys. Lett. 36B, 415 (1971); 36B, 528 (1971).
6. G. Höhler, J. Baacke, H. Schlaile, and P. Sonderegger, Phys. Lett. 20, 79 (1966); G. Höhler, J. Baacke, and G. Eisenbeiss, Phys. Lett. 22, 203 (1966); V. D. Barger and R. J. N. Phillips, Nucl. Phys. B33, 22 (1971).
7. P. D. B. Collins, Phys. Reports (Sec. C of Phys. Lett.), No. 4 (1971).
8. P. D. B. Collins and E. J. Squires, Regge Poles in Particle Physics, in Springer Tracts of Mod. Phys. (Springer-Verlaag, 1968), pp. 72-74.
9. A. A. Anselm and V. N. Gribov, Phys. Lett. 40B, 487 (1972).
10. E. L. Berger and D. Sivers, Phys. Rev. 7D, 2032 (1973).

11. G. F. Chew and D. R. Snider, Phys. Rev. D6, 2057 (1972).
12. G. F. Chew and D. R. Snider, Phys. Rev. D3, 420 (1972).
13. W. R. Frazer and C. H. Mehta, Phys. Rev. D1, 696 (1970).
14. C. Sorensen, Phys. Rev. D6, 2554 (1972).
15. R. Rajaraman, Phys. Rev. Lett. 27, 693 (1971).
16. A. B. Kaidalov, et al., Phys. Lett. 45B, 493 (1973).
17. D. P. Roy and R. G. Roberts, Rutherford Laboratory Pub. RL-74-022, January 1974. See also References therein.
18. G. F. Chew, Phys. Rev. D7, 934 (1973).
19. M. Bishari, G. F. Chew, and J. Koplik, Lawrence Berkeley Laboratory preprint LBL-2129 (1973).
20. For a discussion of the effective pole concept see, Weakly Recurrent Pomerons, G. F. Chew, Review Talk at the Fifth International Conference on High Energy Collisions, Stony Brook, August 1973. For a review of the experimental situation concerning the Pomeron see, Diffractive Processes, David W. G. S. Leith, SLAC-PUB-1330, October 1973; paper submitted to the APS Division of Particles and Fields Meeting, Berkeley, August 1973. See also References therein.
21. J. Finkelstein and K. Kajantie, Nuovo Cimento A56, 659 (1968); G. F. Chew and W. R. Frazer, Phys. Rev. 181, 1914 (1969).
22. H. D. I. Abarbanel, Phys. Rev. D6, 2788 (1972).
23. V. N. Gribov, S. Ya. Pomeranchuk, and K. A. Ter Martirosyan, Phys. Rev. B139, 184 (1965).
24. C. Lovelace, Phys. Lett. 36B, 127 (1971).
25. A. R. White, Nucl. Phys. B50 (1972) 93, 130.
26. A. R. White, NAL-PUB-74/15-THY, January 1974.

27. H. D. I. Abarbanel, G. F. Chew, M. L. Goldberger, and L. H. Saunders, Phys. Rev. Lett. 26, 937 (1971).
28. G. F. Chew and S. D. Ellis, Phys. Rev. D6, 3330 (1972).
29. D. Amati, A. Stanghellini, and S. Fubini, Nuovo Cimento 26, 626 (1962).
30. K. Wilson, Cornell Report CLNS-131 (1970).
31. K. Fialkowski, Phys. Lett. 41B, 379 (1972); W. R. Frazer, R. D. Peccei, S. S. Pinsky, and C.-I Tan, Phys. Rev. D7, 2647 (1973); H. Harari and E. Rabinovici, Phys. Lett. 43B, 49 (1973); C. Quigg and J. D. Jackson, NAL-THY-93 (1972); L. Van Hove, Phys. Lett. 43B, 65 (1973); P. Pirila and S. Pokorski, Phys. Lett. 43B, 502 (1973).
32. W. R. Frazer, D. R. Snider, and C.-I Tan, Phys. Rev. D8, 3180 (1973).
33. J. B. Bronzan, Phys. Rev. D4, 1097 (1971).
34. J. S. Ball and F. Zachariasen, Phys. Lett. 40B, 411 (1972); and University of Utah preprint, December 1973; and Cal Tech Report CALT 68-431.
35. B. R. Desai, P. Kaus, and V. A. Tsarev, Saclay preprint (1973).
36. See the review article of Ref. 20, by David W. G. S. Leith, and References therein.
37. G. F. Chew and J. Koplik, Phys. Lett. 48B, 221 (1974); J. Koplik, Lawrence Berkeley Laboratory report, LBL-2175 (1973), paper submitted to the APS Division of Particles and Fields Meeting, Berkeley, August 1973; Chun-Fai Chan, Chih Kwan Chen, and William Rarita, Phys. Lett. 47B, 512 (1973).

38. E. Leader and U. Maor, Phys. Lett. 43B, 505 (1973); S. Barshay and V. Rostokin, Phys. Rev. D8, 2867 (1973); Shigeo Minami, Osaka City University; Sumiyoshi-ku, Osaka, August (1973).

39. V. N. Gribov and A. A. Migdal, Soviet J. Nucl. Phys. 8, 703 (1969).

40. J. L. Cardy and A. R. White, CERN preprint, Ref. TH 1740-CERN, September 1973.

41. J. B. Bronzan, NAL-PUB-73/69-THY, September 1973.

42. H. D. I. Abarbanel and J. B. Bronzan, NAL-PUB-73/90-THY, December 1973, and NAL-PUB-73/91-THY, December 1973.

43. R. C. Brower and J. H. Weis, Phys. Lett. 41B, 631 (1972); and "Pomeron Couplings" Cal. Tech.-Washington preprint (1973).

44. L. Caneschi and A. Pignotti, Phys. Rev. 184, 1915 (1969).

45. In performing this calculation we closely follow M. L. Goldberger, Multiperipheral Models and High Energy Processes, Princeton University preprint, PURC 4159-42, July 1971, p. 75.

46. G. Höhler, H. P. Jakob, and P. Kroll, Z. Physik 261, 401 (1973).

47. R. Shankar, UCB preprint LBL-2678 (1974). Submitted to Phys. Lett. B.

FIGURE CAPTIONS

Fig. 1. The discontinuity of $B(j,t = 0)$ across the cut for the case when R is a Pomeron. For purposes of relative normalization the rectangle centered at $j = \alpha_P(0)$ has been given an area corresponding to the Pomeron residue.

Fig. 2. The slope parameter of the proton-proton elastic differential cross section as function of t for $\ell n\, s = 8$. The straight line is the unperturbed value. The date points are from Barbiellini, et al.[1]

Fig. 3. Similar plot to Fig. 2 for $\ell n\, s = 6$.

Fig. 4. The slope parameter of the proton-proton elastic differential cross section as function of $\ell n\, s$ for $t = 0$.

Fig. 5. Similar plot to Fig. 1 for the case when R is a rho.

Fig. 6. The effective rho trajectory: (i) ——— at $\ell n\, s = 5$; (ii) ------ at $\ell n\, s = 3$. The straight line is the unperturbed trajectory $\alpha_\rho{}^0(t) = 0.55 + t$. The data point at $t = 0$ is the Serpukhov result. The data points at $t \lesssim 0$ are from Ref. 46 and correspond to $\ell n\, s \sim 2 - 3.5$.

Fig. 7. The intercept of the effective rho trajectory as function of $\ell n\, s$.

Fig. 8. The Pomeron-omega-omega triple Regge vertex in the Multiperipheral Model.

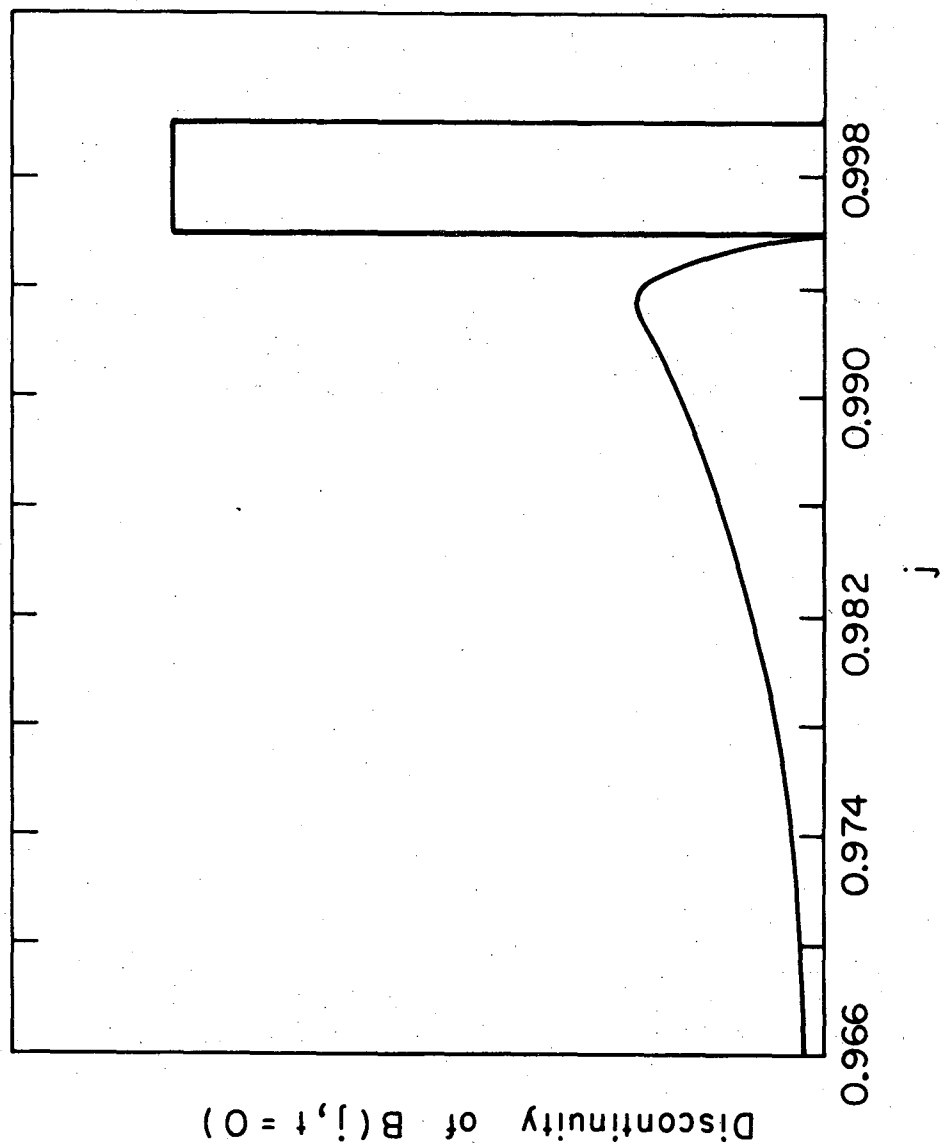

XBL744-2964

Fig. 1

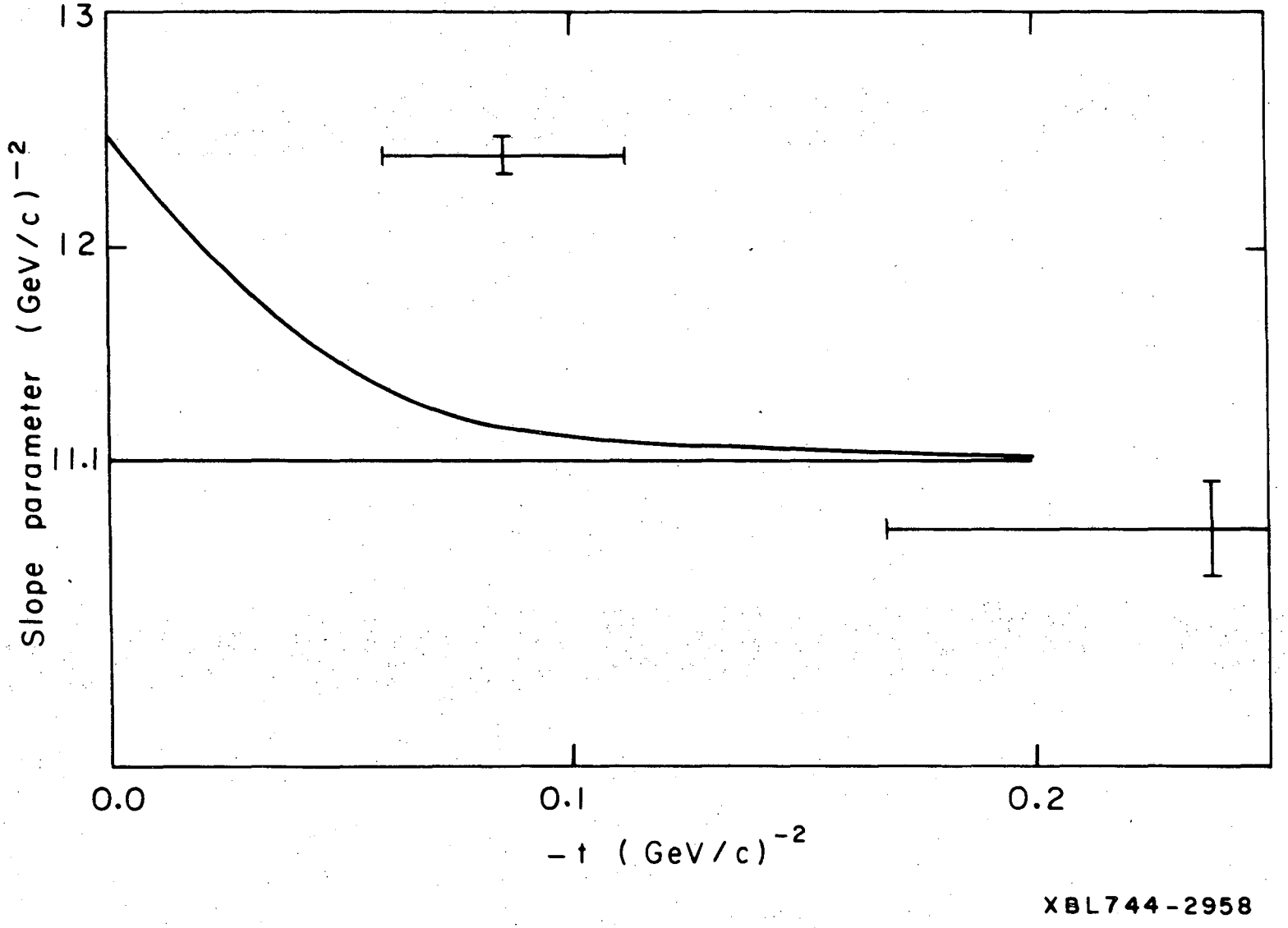

Fig. 2

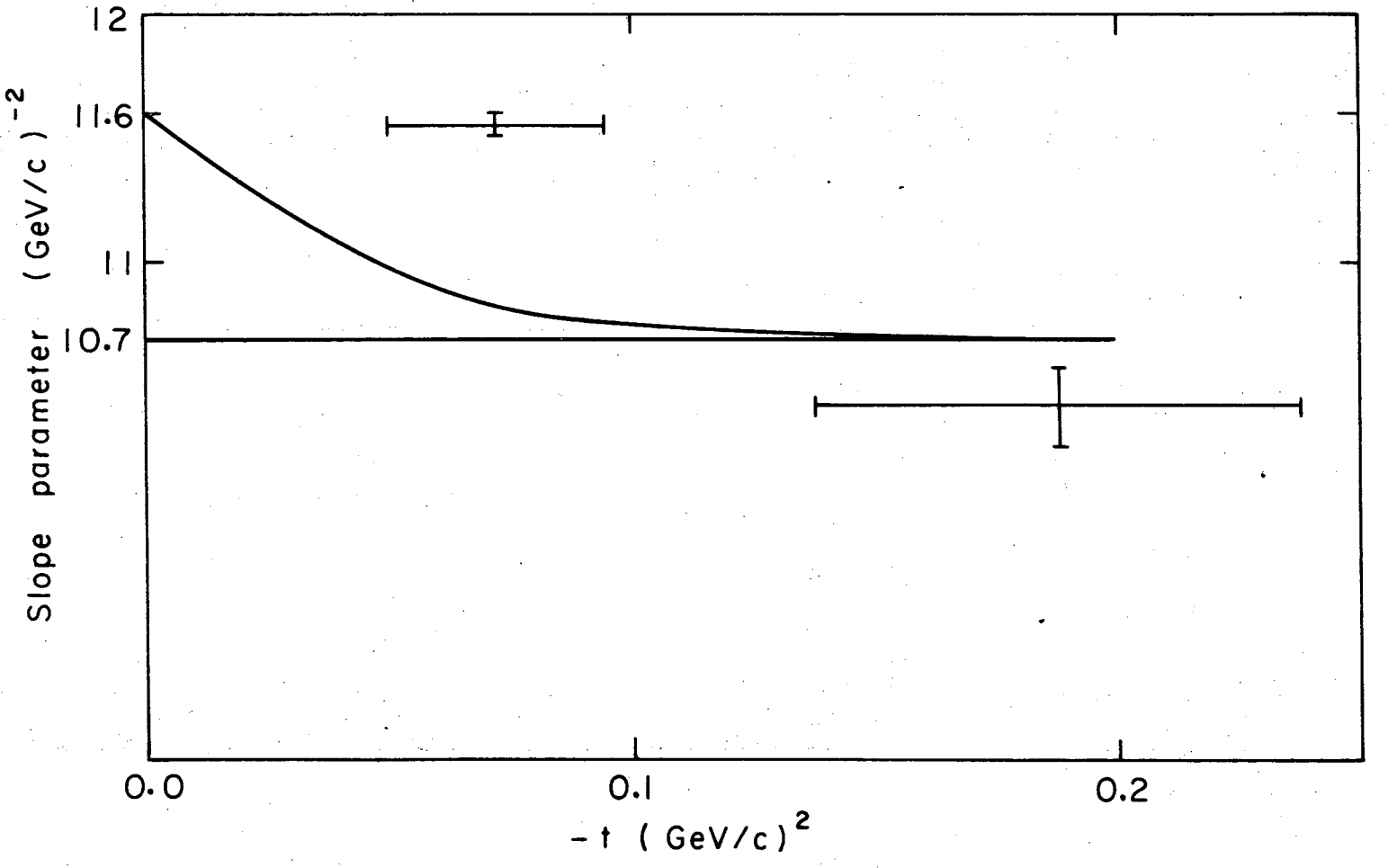
12
11.6
11
10.7
Slope parameter (GeV/c)$^{-2}$
0.0
0.1
0.2
$-t$ (GeV/c)^2
XBL744-2959

Fig. 3

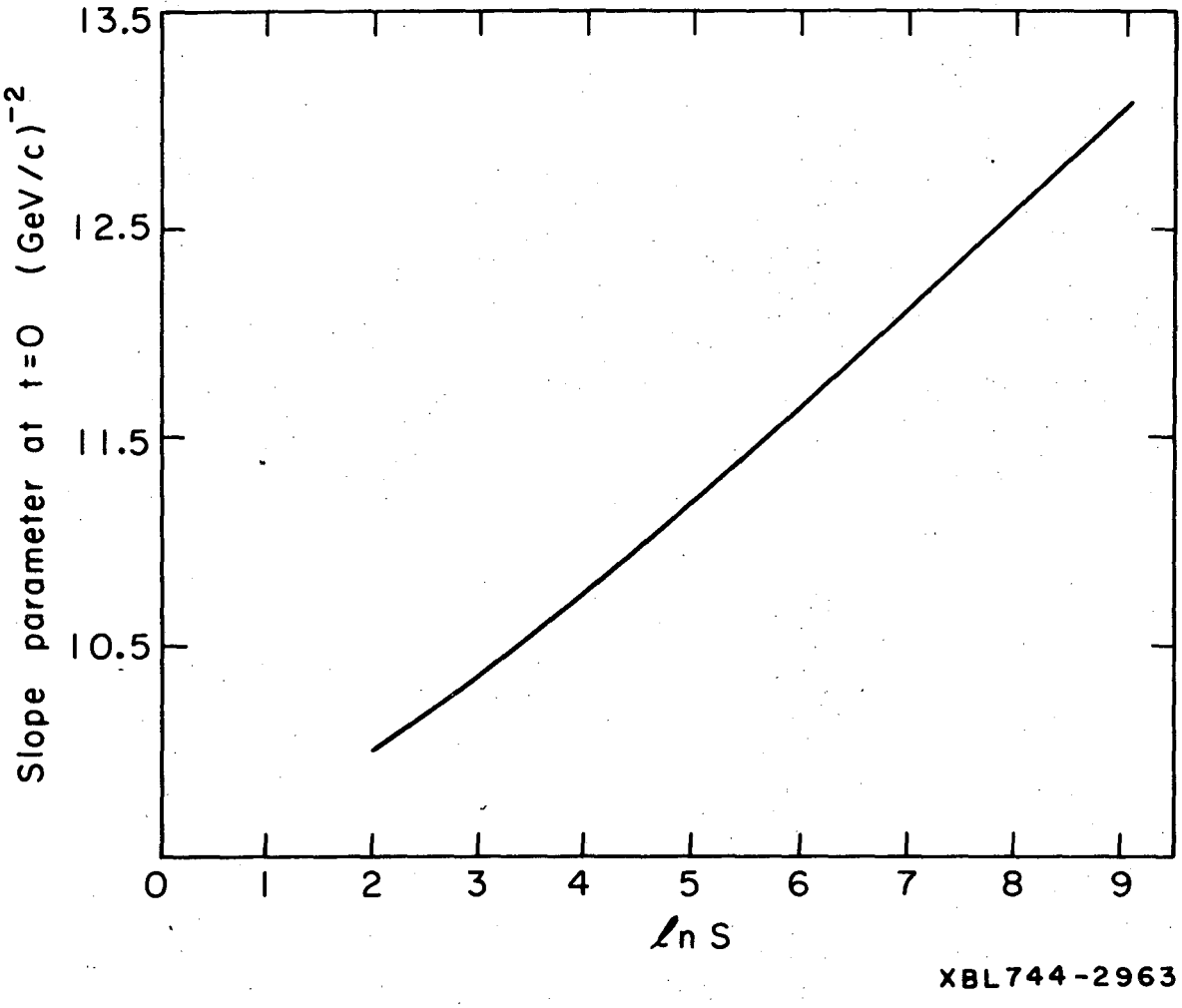
13.5
12.5
11.5
10.5
Slope parameter at t=0 (GeV/c)$^{-2}$
0
1
2
3
4
5
6
7
8
9
ℓn S
XBL744-2963

Fig. 4

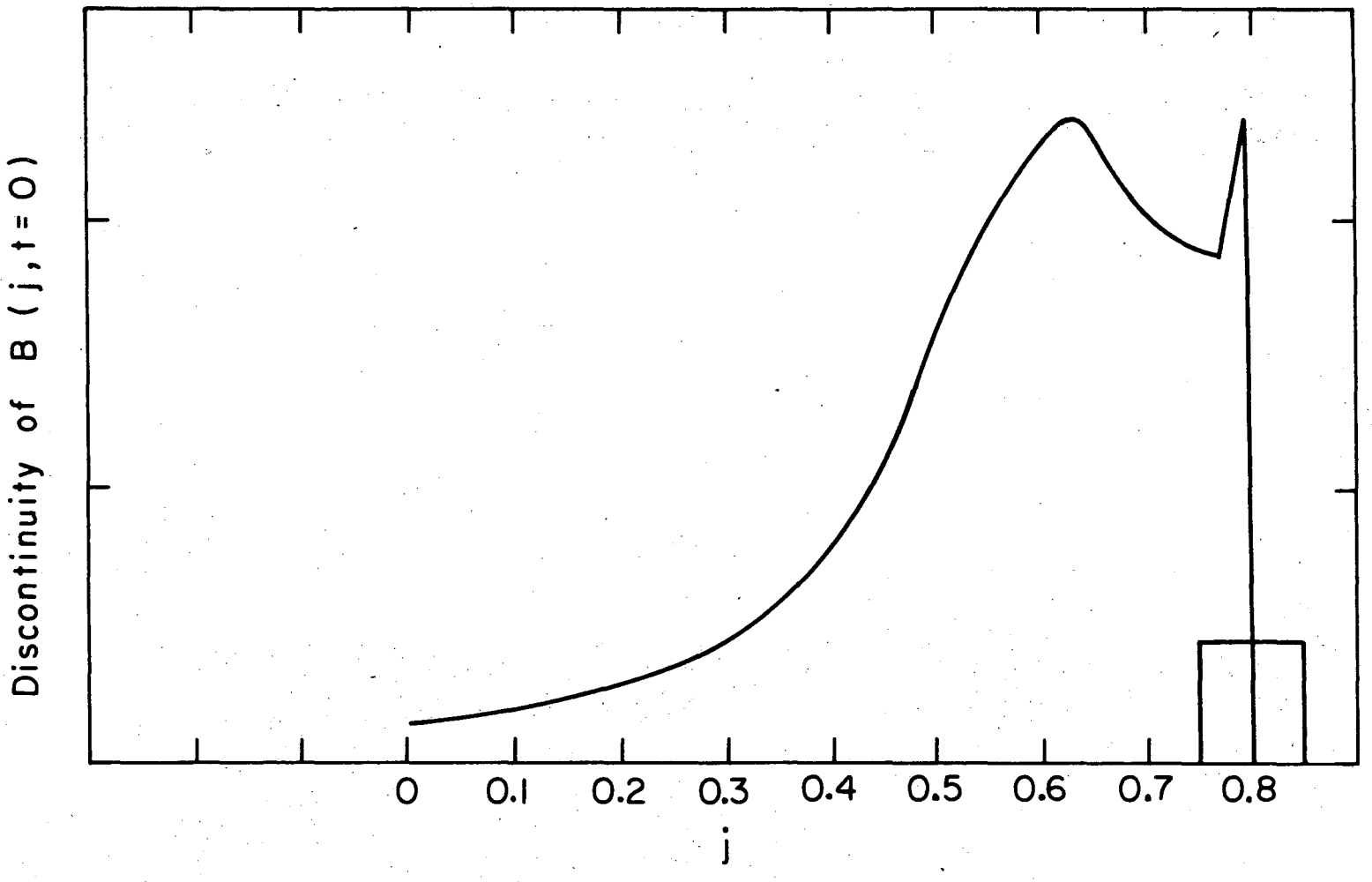

XBL 744-2961

Fig. 5

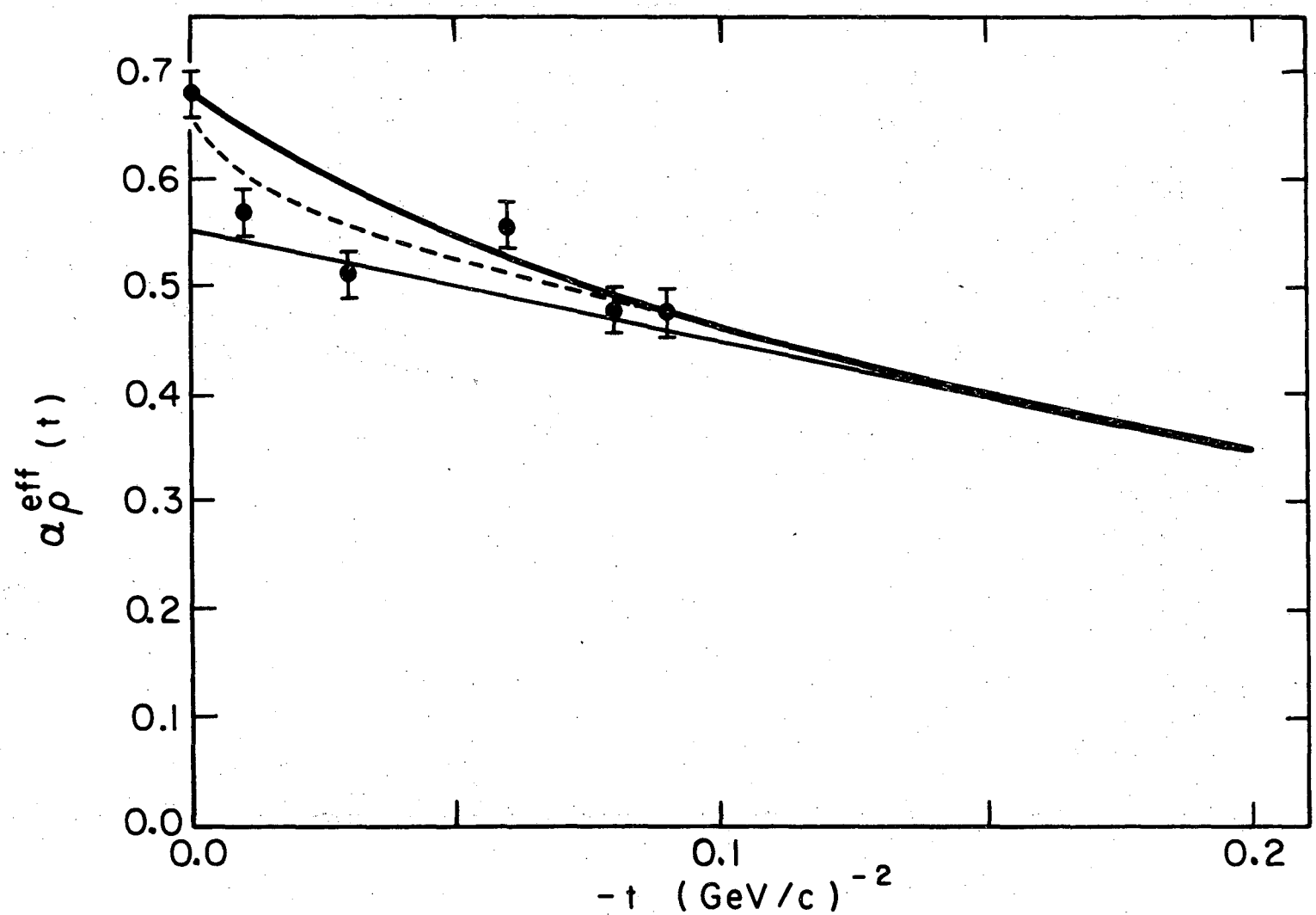

XBL744-2957

Fig. 6

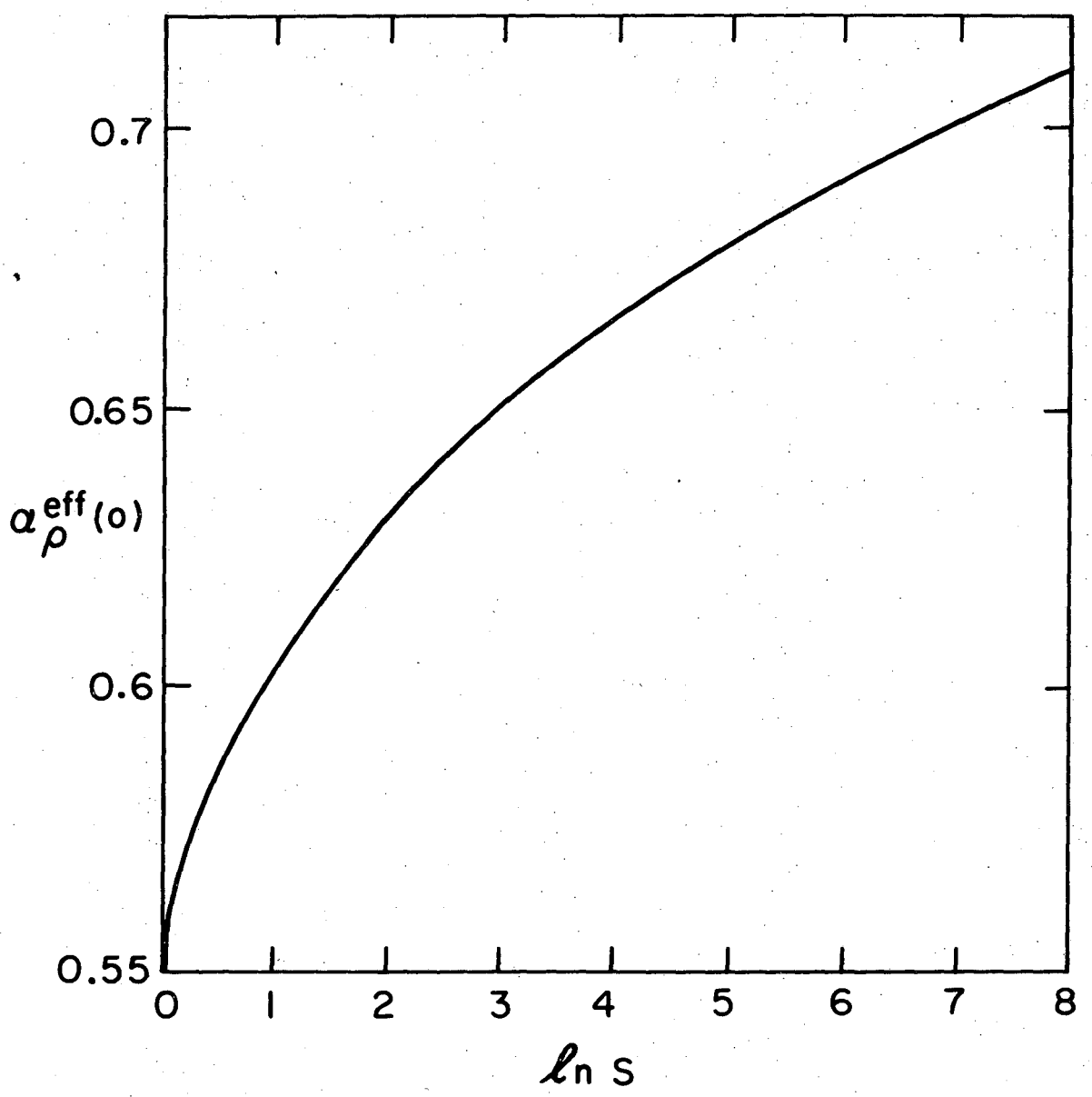

XBL744-2962

Fig. 7

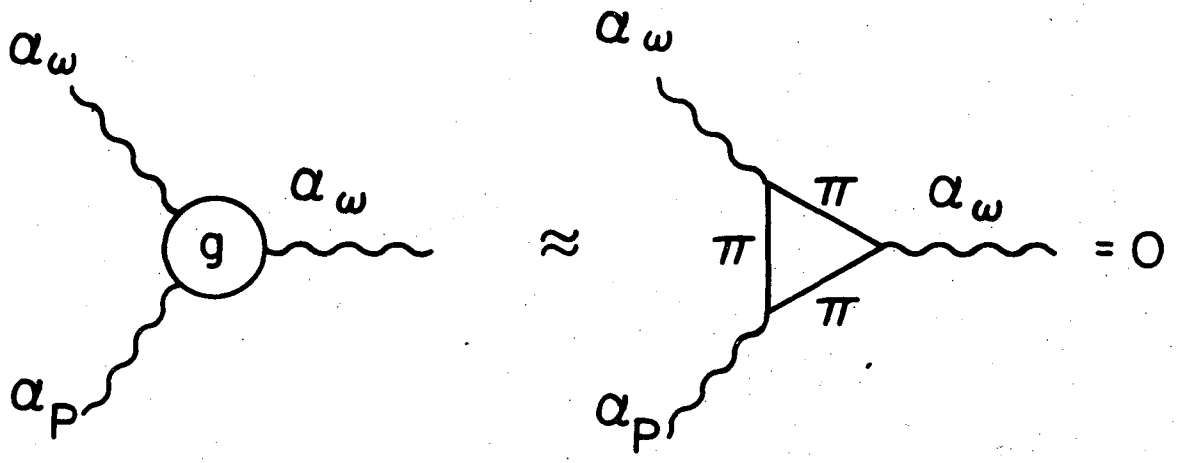

XBL744-2960

Fig. 8

TECHNICAL INFORMATION DIVISION
LAWRENCE BERKELEY LABORATORY
UNIVERSITY OF CALIFORNIA
BERKELEY, CALIFORNIA 94720